ELSEVIER

Contents lists available at ScienceDirect

# Experimental Cell Research

journal homepage: www.elsevier.com/locate/yexcr





# Fatty acid binding protein 3 deficiency limits atherosclerosis development via macrophage foam cell formation inhibition

Lili Tan <sup>a,b,1,\*</sup>, Jie Lu <sup>b,1</sup>, Limin Liu <sup>b</sup>, Lu Li <sup>b</sup>

- a Department of Cardiology, The Central Hospital Affiliated to Shenyang Medical College, Shenyang, Liaoning, People's Republic of China
- b Department of Cardiology, The Second Affiliated Hospital of Shenyang Medical College, Shenyang, Liaoning, People's Republic of China

#### ARTICLE INFO

Keywords: Atherosclerosis FABP3 Macrophage Foam cell formation PPARy

#### ABSTRACT

Atherosclerosis is the underlying contributing factor of cardiovascular disease, which is a process of inflammation and lipid-rich lesion. Macrophage-derived foam cell is a key hallmark of atherosclerosis and connected with various factors of lipid metabolism. Here, we showed that fatty acid binding protein 3 (FABP3) was upregulated in the aorta of  $ApoE^{-/-}$  mice with high-fat-diet (HFD) feeding. Knockdown of FABP3 in HFD-fed  $ApoE^{-/-}$  mice notably facilitated cholesterol efflux, inhibited macrophage foam cell formation, and thus prevented atherogenesis. Furthermore, FABP3 silencing decreased the expression of peroxisome proliferator-activated receptor  $\gamma$  (PPAR $\gamma$ ). Mechanistic studies had disclosed the involvement of PPAR $\gamma$  signaling in balancing cholesterol uptake and efflux and diminishing foam cell formation. These findings firstly revealed an anti-atherogenic role of FABP3 silencing in preventing foamy macrophage formation partly through PPAR $\gamma$ , which might be a beneficial approach for therapying atherosclerosis.

# 1. Introduction

Atherosclerosis is the most common vascular disease worldwide characterized by progressive inflammation, lipid-driven vascular lesions, which is a leading cause of threat to human health [1]. Macrophage foam cell formation is a prominent hallmark of atherosclerosis. During atherosclerosis progression, excess cholesterol and saturated fatty acid lead to lipid droplets accumulation in the endothelium. In the meanwhile, inflammation and shear stress promote endothelial cells to recruit mononuclear cells that aggregate in the endothelium of blood vessels. Then, the mononuclear cells differentiate into macrophages and subsequently form foam cells through uptaking oxidized low-density lipoproteins (ox-LDL) [2,3]. After that, the necrosis of the lipid-rich lesion will be formed when the foam cells die and the atheromatous plaque will be taking form. Once the plaque rupture, it will induce platelet deposition and thrombosis, and cause stroke and heart attack [4]. Hence, restraining macrophage foam cell formation is an appropriate treatment strategy to relieve atherosclerosis.

Fatty acid binding protein (FABP) is discovered by Ockner and coauthors in 1972 and strongly linked to lipid metabolism [5]. FABP3 is a member of the FABP family, which is expressed in a wide range of tissue types, such as brain, skeletal muscle, aorta, and so on [6]. FABP3 was reported rapidly released from myocardial cells into the circulation in chronic heart failure patients and proposed as a sensitive biological marker for the evaluation of myocardial injury [7]. Serum FABP3 levels were elevated in patients with nonalcoholic fatty liver disease, which indicated that FABP3 was a marker of subclinical atherosclerosis [8]. Furthermore, FABP3 was associated with vascular disease. FABP3 presented a high level in plasma of the patients with peripheral arterial disease which exacerbated the situation [9]. Remarkably, the mRNA level of FABP3 in macrophages was upregulated with the response of Chlamydia pneumoniae and Porphyromonas gingivalis at the time of macrophage foam cell formation [10]. Overexpression of FABP3 promoted inflammation and synchronously accelerated human vascular smooth muscle cell growth and migration [11]. Nevertheless, research on the effects of FABP3 on foam cell formation in atherosclerosis is rare.

Peroxisome proliferator-activated receptors (PPARs) are a group of nuclear receptors of the ligand-activated transcription factors that are related to inflammation and the metabolism of lipids [12]. PPAR $\gamma$ , one of the PPARs, has the ability to regulate cholesterol distribution and efflux. The expression of PPAR $\gamma$  was upregulated in oxidized low-density lipoprotein (ox-LDL) treated-monocytes, which played an important role

<sup>\*</sup> Corresponding author. Department of Cardiology, The Central Hospital Affiliated to Shenyang Medical College, No. 5, Nanqi West Road, Tiexi District, Shenyang, Liaoning, PR China.

E-mail address: tanlili123@163.com (L. Tan).

<sup>&</sup>lt;sup>1</sup> The authors contributed equally to this work.

in the differentiation of macrophages to foam cells [13]. On the contrary, the number of foamy macrophages induced by myelin was increased within the downregulated expression of PPAR $\gamma$  under multiple sclerosis-associated pro-inflammatory cytokines [14]. Moreover, a previous study had reported the connection between the FABP family and PPAR $\gamma$ . FABP4, another member of the FABP family, enhanced PPAR $\gamma$  activation and elevated triglyceride (TG) concentrated in macrophages [15]. We hypothesized that FABP3 might play an important role via PPAR $\gamma$  in atherosclerosis.

In this current study, we first measured the expression of FABP3 in the atherosclerosis mouse model, subsequently generated FABP3 silencing  ${\rm ApoE}^{-/-}$  mice *in vivo* and knockdown of FABP3 murine peritoneal macrophages *in vitro* and studied the effects of FABP3 on foam cell formation in atherosclerosis occurrence and development.

#### 2. Material and methods

#### 2.1. Animal studies

Eight-week-old male apolipoprotein E-knockout (ApoE $^{-/-}$ ) mice were purchased from Beijing HFK Bioscience CO., LTD (Beijing, China) and fed with high-fat-diet (HFD), which was containing 21 % pork fat and 0.5 % cholesterol (Junke Biological Co., LTD, Nanjing, China) for 12 weeks [16]. C57BL/6J mice were fed with common forage as the control. For experiments, ApoE $^{-/-}$  mice were also given an intravenous injection of 4  $\times$  10 $^7$  TU lentivirus carrying shFABP3 or shRNA NC (FENGHUISHENGWU, Changsha, China) into the tail vein on the first day of HFD feeding and repeated 6 weeks later. During the experiments, body weight measurements were performed weekly. After 12 weeks of HFD, the mice were weighed and the blood was drawn, and then the mice were sacrificed for subsequent aorta sample detecting. The experimental procedures were approved by the Ethics Committee of Shenyang Medical College.

# 2.2. Histology analysis

The aortic root tissues were embedded by optimal cutting temperature compound and sliced into serial 10- $\mu m$  frozen sections. For histopathologic change accessing, the sections were stained with hematoxylin (H8070, Solarbio, Beijing, China) and eosin (A600190, Sangon, Shanghai, China). For lesion development evaluation, oil red O (O0625, Sigma-Aldrich, St Louis, USA) staining was performed in the aortic root sections. Images were captured with the Olympus BX53 microscope with the Olympus DP73 camera (Tokyo, Japan) at 40  $\times$  magnification.

# 2.3. Immunofluorescence and immunohistochemistry staining

The aortic root sections were treated with tissue antigen recovery, blocked with goat serum, and incubated with the primary antibodies anti-Mac-3 (66301-1-Ig, Proteintech, Rosemont, USA) and FABP3 (A8789, ABclonal, Wuhan, China) at 1: 200 dilution overnight at 4  $^{\circ}$ C. Subsequently, secondary antibodies contained Cy3-labeled Goat Anti-Rabbit IgG (1: 200, A0516, Beyotime, Shanghai, China) and FITC-labeled Goat Anti-Mouse IgG (1: 200, A0568, Beyotime) were used for fluorescing at room temperature for 1 h. For immunohistochemistry, anti-Mac-3 (1: 100, Proteintech) was used as the primary antibody and horseradish peroxidase (HRP) conjugated goat anti-mouse IgG (1: 500, 31,430, ThermoFisher, Waltham, USA) was used as the secondary antibody. The sections were counterstained with DAPI or hematoxylin for immunofluorescence and immunohistochemistry and recorded using the Olympus microscope (BX53) with the Olympus camera (DP73) under 400  $\times$  magnification.

**Table 1** Antibody information.

Antibody	Dilution	Supplier	NO.	Country
FABP3 antibody	1: 500	Abclonal	A8789	China
PPARγ antibody	1: 1000	Abclonal	A0270	China
LXRα antibody	1: 1000	Abclonal	A3974	China
CD36 antibody	1: 1000	Abclonal	A19016	China
SRA1 antibody	1: 1000	Affinity	AF6330	USA
SRB1 antibody	1: 500	Abclonal	A0827	China
ABCA1 antibody	1: 1000	Affinity	DF8233	USA
ABCG1 antibody	1: 500	Abclonal	A17907	China
Rabbit Anti-Goat IgG-HRP	1: 3000	Solarbio	SE238	China
Goat Anti-Rabbit IgG-HRP	1: 3000	Solarbio	SE134	China
Goat Anti-Mouse IgG-HRP	1: 3000	Solarbio	SE131	China

### 2.4. Plasma lipid levels

Murine plasma triglyceride (TG), total cholesterol (TC), high-density lipoprotein (HDL), and low-density lipoprotein (LDL) were examined by using commercial kits from Nanjing Jiancheng Bioengineering Institute (TG, A110-1; TC, A111-2; HDL, A112-2; LDL, A113-1) following the manufacturer's instructions.

### 2.5. Cell culture and infection

Murine peritoneal macrophages were purchased from Procell (Wuhan, China) maintained in the special culture medium (Procell) at 37  $^{\circ}\text{C}$  in a 5 % CO $_2$  atmosphere. The cells were seeded in culture dishes and infected with lentivirus carrying shFABP3 or shRNA NC (FENGHUISHENGWU) according to the manufacturer's protocols for 24 h. After that, ox-LDL (50  $\mu\text{g/ml}$ , Peking Union-Biology, Beijing, China) was added for 24 h to establish a macrophage model of lipid accumulation. In addition, 1  $\mu\text{mol/L}$  Rosiglitazone (a PPAR $\gamma$  agonist, R128083, Aladdin, Shanghai, China) or 10  $\mu\text{mol/L}$  GW9662 (an irreversible PPAR $\gamma$  antagonist, HY-16578, MedChemExpress, Shanghai, China) was added simultaneously with ox-LDL for further experiments.

### 2.6. Western blotting analysis

Cells or tissues were lysed using RIPA buffer (R0010, Solarbio). The

**Table 2** Oligonucleotide primers for qPCR

Gene	Sequences (5′-3′)	Product Size (bp)	Gene ID
ABCA1	GCAACAGATGCCCTACCC	183	NM_013454.3
ABCA1 R	ATGCCATTGTCCAGACCCA		
ABCG1	GGGAACGAAGCCAAGAAG	292	NM_009593.2
ABCG1	TACCCAGAGCAGCGAACA		
CD36 F CD36 R	ACTGTGGGCTCATTGCT CTTGGCTAGATAACGAACT	284	NM_001159558.1
FABP3 F FABP3	ACCAAGCCTACTACCATCA TCACGCCTCCTTCTCAT	294	NM_010174.2
R	10/10000110110/11		
LXRα F LXRα R	GGGCAGTACCGCAACGA CTCACGGATGGCACTCACA	192	NM_009696.4
PPARγ F PPARγ	ACCACTCGCATTCCTTT CACAGACTCGGCACTCA	264	NM_001127330.2
R SRA1 F	CCTCTGGAACAGGCATTG	119	NM_025291.3
SRA1 R SRB1 F SRB1R	GGTATTGACAACTTCCCTCC ATCTGGTGGACAAATGGAA GAAGCGATACGTGGGAAT	209	NM_016741.2
β-actin F β-actin R	CTGTGCCCATCTACGAGGGCTAT TTTGATGTCACGCACGATTTCC	155	NM_007393.5

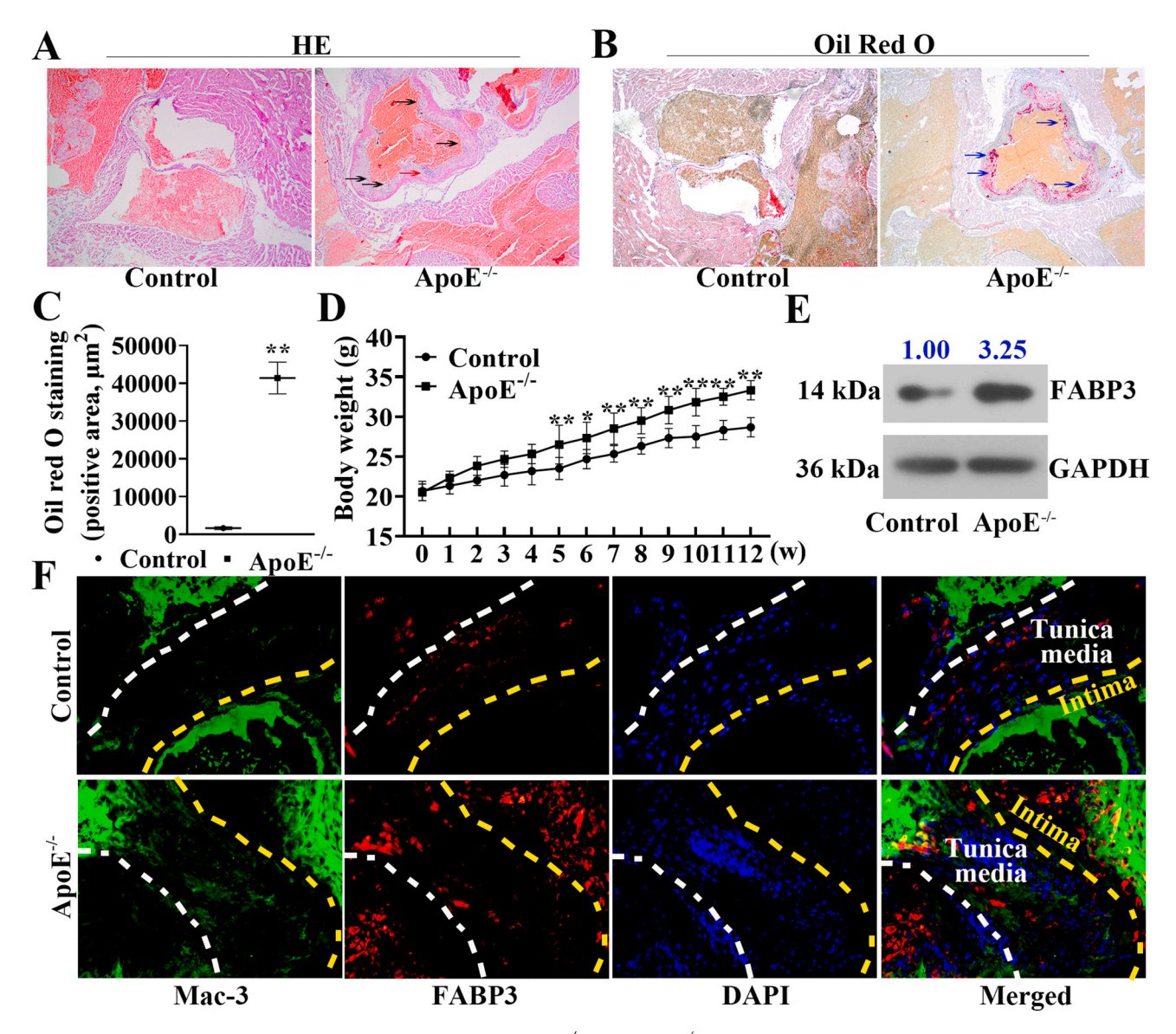


Fig. 1. FABP3 was highly expressed in the aortic tissues of HFD-fed ApoE $^{-/-}$  mice. ApoE $^{-/-}$  mice were fed with HFD for 12 weeks and C57BL/6J mice were fed with common forage as the control. Representative images of aortic root for (A) HE staining, 40 × and (B) Oil Red O staining, 40 × . (C) Quantification of Oil Red O staining, (D) Bodyweight measurements were performed weekly. (E) Western blot of FABP3 and (F) Immunofluorescence of FABP3 and Mac-3 in the aortic root of HFD-fed ApoE $^{-/-}$  mice and C57BL/6J mice, 400 × . \*p < 0.05, \*\*p < 0.01 denote significant differences between the Control and the ApoE $^{-/-}$  mice.

protein concentration was quantified with BCA Protein Assay Kit (PC0020, Solarbio). An equal amount of protein was resolved by electrophoresis on 8 %, 10 %, and 15 % SDS-PAGE and then transferred onto the PVDF membrane (IPVH00010, Millipore, Billerica, USA). After blocking the PVDF membranes with 5 % skim milk at room temperature for 1 h, the membranes were incubated with the appropriate primary antibodies, followed by incubation with the secondary antibodies (Table 1). The protein bands were observed with the ECL Western Blotting Substrate (PE0010, Solarbio). GAPDH was used as the internal reference.

# 2.7. Quantitative polymerase chain reaction (qPCR)

Total mRNA was extracted from murine peritoneal macrophages or aorta tissues by using TRIpure (RP1001, BioTeke, Beijing, China) and reverse-transcribed into cDNA using BeyoRT II M-MLV (D7160L, Beyotime) with RNase inhibitor supplementary (RP5602, BioTeke). All qPCR reactions were performed on a Real-Time Quantitative Thermal Block (Exicycler 96, Bioneer, Korea) and GAPDH was regarded as a

reference gene. The sequences of the genes were synthesized by Gensceript and illustrated in Table 2.

# 2.8. Statistical analysis

All the experiments were repeated six times *in vivo* and repeated three times *in vitro*. Results were represented as Means  $\pm$  SD. One-way ANOVA with multiple comparisons test or two-tailed unpaired *t*-test was used to analyze the data (Graphpad Prism 8.0, San Diego, CA). The *p* values < 0.05 were considered significant.

# 3. Results

# 3.1. FABP3 showed overexpression in the aortic tissues of HFD-fed $ApoE^{-/-}$ mice

To investigate the effect of FABP3 on atherosclerosis, we first established the atherosclerotic model with HFD feeding in ApoE<sup>-/-</sup> mice for 12 weeks. As demonstrated in Fig. 1A, atherosclerotic lesion

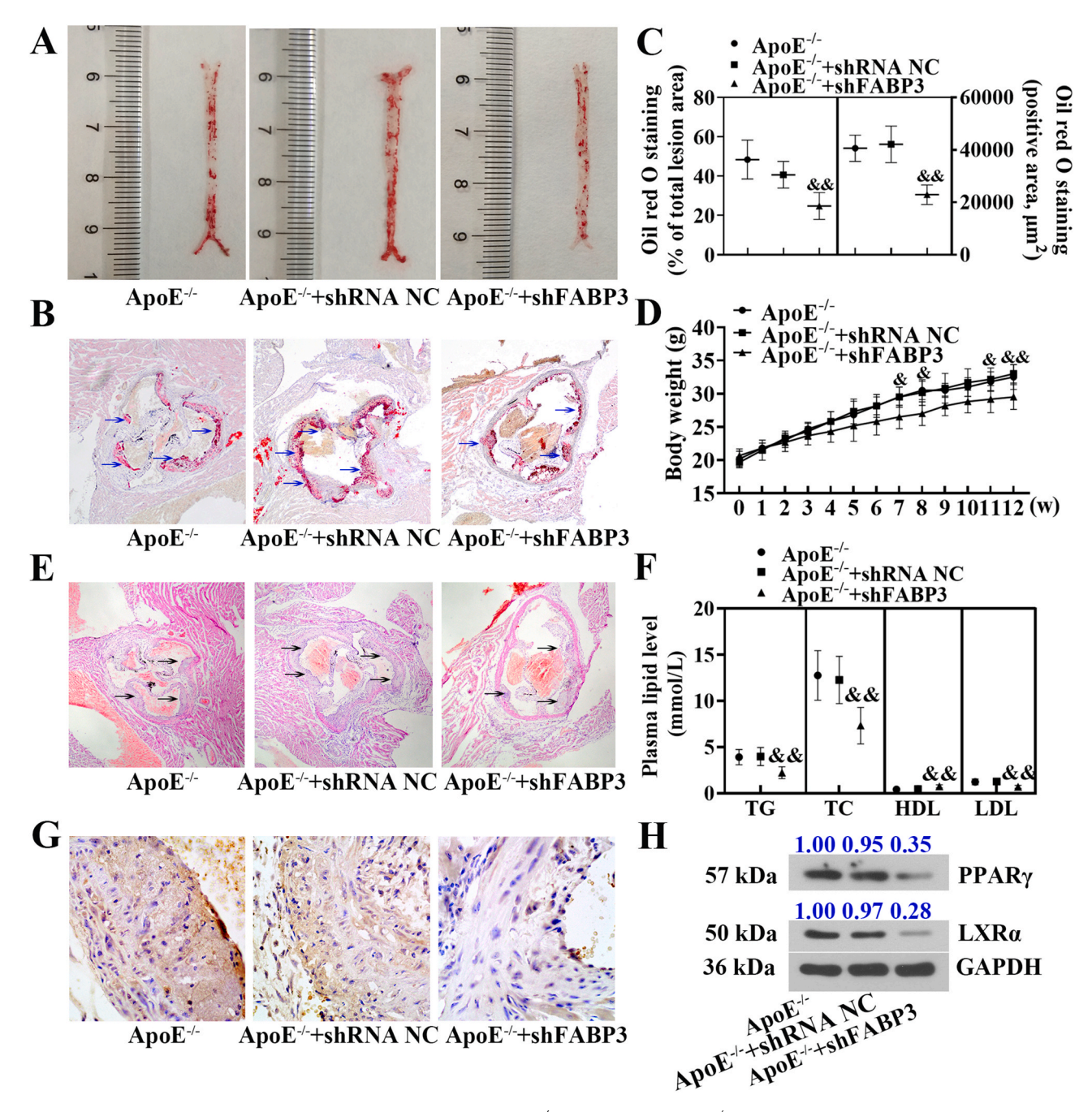


Fig. 2. Silencing FABP3 lessened atherosclerotic lesions in HFD-fed ApoE $^{-/-}$  mice. HFD-fed ApoE $^{-/-}$  mice were treated with intravenous injection of caudal veins with lentivirus carrying shFABP3 or shRNA NC (4 × 10 $^7$  TU) on the first day of HFD feeding and repeated on day 43. (A, C) Over 12 weeks, aortas were isolated for detecting by Oil Red O staining in en face. The staining was quantified by image analysis protocol. (B, C) Oil Red O staining followed by quantitative analysis of aortic root, 40 × . (D) Examination of body weights and (F) serum TG, TC, HDL, and LDL in HFD-fed ApoE $^{-/-}$  mice infected with lentivirus carrying shFABP3 or shRNA NC. (E) Representative images of aortic root for HE staining, 40 × . (G) Representative images of Mac-3 staining by immunohistochemistry in the aortic root. (H) Western blot analysis of PPARγ and LXRα in the aorta.  $^{\&}p < 0.05$ ,  $^{\&\&}p < 0.01$  denote significant differences between the ApoE $^{-/-}$  shRNA NC mice and ApoE $^{-/-}$  shFABP3 mice.

formation was observed in the aortic root of ApoE $^{-/-}$  mice with obvious fibrous cap (shown with the black arrow) and necrosis (shown with the red arrow). Accordingly, Fig. 1B and C showed that lipid deposition in plaques was distinctly presented in the ApoE $^{-/-}$  mice with HFD (shown with the blue arrow, P < 0.01). Moreover, the weights of ApoE $^{-/-}$  mice were increased significantly than that in the control (Fig. 1D, P < 0.05). These results displayed that the atherosclerotic model was established successfully. Subsequently, the protein level of FABP3 in the aortic root of ApoE $^{-/-}$  mice was detected which was increased to more than three times in aortas from ApoE $^{-/-}$  mice (Fig. 1E). Notably, the expression of

Mac-3 was elevated and partly co-expressed with FABP3 (Fig. 1F).

# 3.2. FABP3 knockdown alleviated atherosclerotic lesions in HFD-fed ApoE $^{-/\cdot}$ mice

To explore the effect of FABP3 on atherosclerotic plaque formation, we established the ApoE $^{-/-}$  mice model of atherosclerosis by feeding HFD over 12 weeks and given an intravenous injection of FABP3 shRNA lentivirus. In line with expectations, the protein level of FABP3 was decreased in the mouse aortas after interference with the lentivirus-

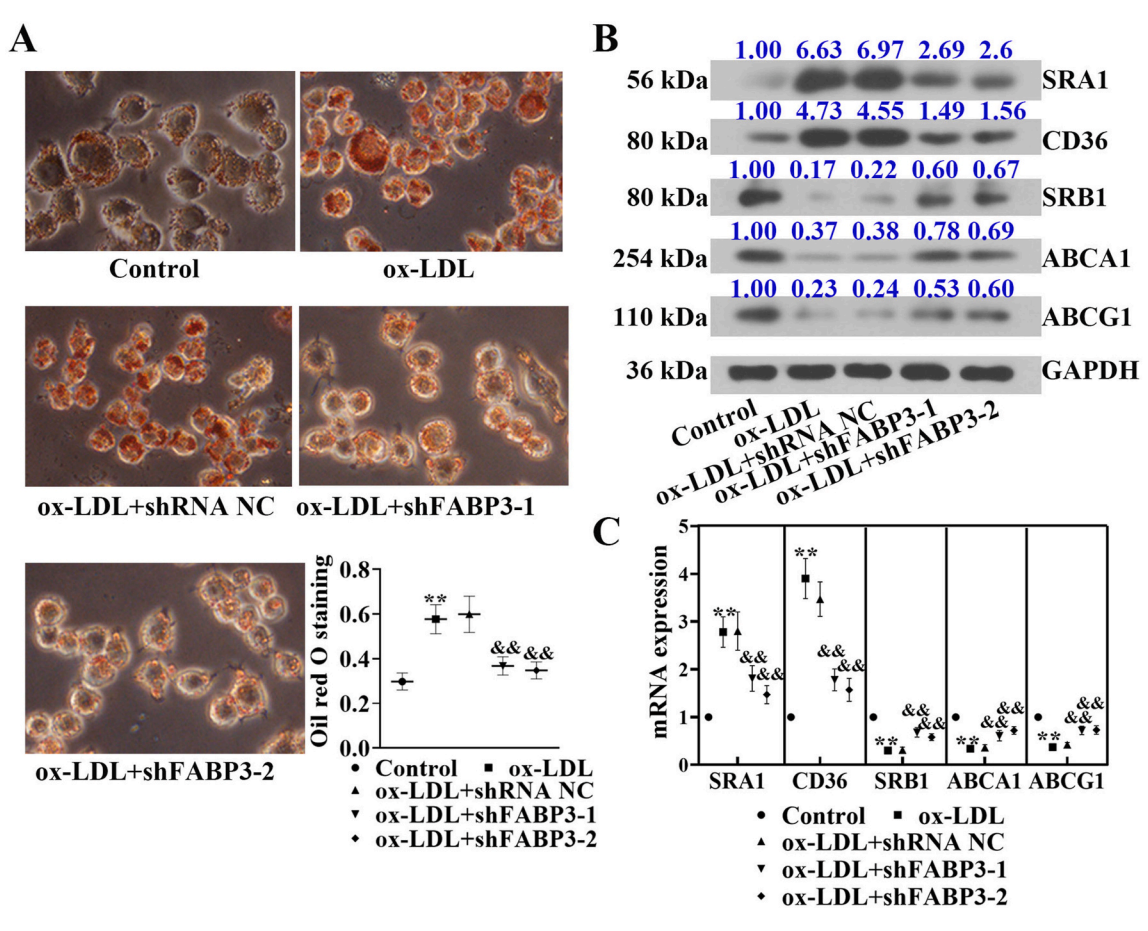


Fig. 3. FABP3 knockdown reduced macrophage foam cell formation. Murine peritoneal macrophages were maintained in the special culture medium at 37 °C in a 5 % CO<sub>2</sub> atmosphere. The cells were infected with lentivirus carrying shFABP3 or shRNA NC for 24 h and subsequently exposed with ox-LDL (50  $\mu$ g/ml) for 24 h. (A) Representative Oil Red O-stained images of macrophages and quantification of the staining. (B) Immunoblots of SRA1, CD36, SRB1, ABCA1, and ABCG1 in macrophages. (C) Quantification of relative mRNA expression of SRA1, CD36, SRB1, ABCA1, and ABCG1. \*\*p < 0.01 denote significant differences between the Control and the ox-LDL groups, \* $^{\&\&}p < 0.01$  denote significant differences between the ox-LDL shRNA NC and ox-LDL + shFABP3 groups.

mediated FABP3 shRNA (Supplementary Figure 1). Images of oil red O staining of aortas showed lipid deposition in plaques had a 40 % reduction in lesion area compared with ApoE $^{-/-}$ shRNA NC mice (Fig. 2A and Fig. 2C, p < 0.01). Similar results were obtained in the aortic root tissues with oil red O staining (Fig. 2B and C, shown with the blue arrow, p < 0.01). Fig. 2E exhibited the decrease of the fibrous cap (shown with the black arrow) and atherosclerotic lesion in the aortic root of ApoE $^{-/-}$ mice that received the FABP3 shRNA lentivirus than that of control. Meanwhile, the body weight and serum levels of TG, TC, and LDL in ApoE $^{-/-}$ shRNA NC mice were inhibited by FABP3 shRNA lentivirus administration (Fig. 2D and F). Moreover, levels of Mac-3, PPAR $\gamma$ , and liver X receptor  $\alpha$  (LXR $\alpha$ ) were noticed to decrease in the aortas of ApoE $^{-/-}$ shFABP3 mice (Fig. 2G and H).

# 3.3. Depletion of FABP3 reduced foamy macrophages formation

In order to unveil the functional roles of FABP3 in atherosclerosis, knockdown of FABP3 in murine peritoneal macrophages exposed with ox-LDL were performed. Both mRNA and protein levels of FABP3 were downregulated in the macrophage infected with the lentivirus-mediated FABP3 shRNA (Supplementary Figure 2). Fig. 3A exhibited that downregulation of FABP3 reversed the foam cell formation in macrophages induced by ox-LDL. In line with the observations, depletion of FABP3 counteracted the changes of protein markers of lipid metabolism caused by ox-LDL, manifested as reduced the expression of scavenger receptor 1 (SRA1) and CD36, factors responsible for the uptake of lipoproteins, whereas facilitated the level of scavenger receptor class B type 1 (SRB1),

ATP-binding cassette transporter A1 (ABCA1), and ATP-binding cassette transporter G1 (ABCG1), transporters responsible for efflux of cholesterol (Fig. 3B). Besides, qPCR results were as expected consistent with the protein analysis (Fig. 3C). These findings suggested that FABP3 silencing lessened the formation of lipid-laden macrophages.

# 3.4. FABP3 downregulation diminished foamy macrophages formation correlated with PPARy signal pathway

Since PPAR $\gamma$  and LXR $\alpha$  were closely related to lipid metabolism, they especially, played a key role in the foam cell formation [17]. We further performed a Western blot to detect the protein expression of PPAR $\gamma$  and LXR $\alpha$  in ox-LDL-treated murine peritoneal macrophages with FABP3 silencing. Levels of PPAR $\gamma$  and LXR $\alpha$  were increased in the ox-LDL group compared with the control group, but dramatically reduced by FABP3 knockdown (Fig. 4A). These findings were further convinced by qPCR (Fig. 4B, P < 0.05). Moreover, silencing FABP3 could decrease ox-LDL-induced foam cell formation of murine peritoneal macrophages. Interestingly, rosiglitazone could reverse the reduction of macrophage foam cell formation that resulted from FABP3 downregulation (Fig. 4C). It was worth noting that rosiglitazone promoted the expression of LXR $\alpha$  and CD36, and further elevated the SRB1, ABCA1, and ABCG1 level, which was shown in Fig. 4D. However, GW9662 had the opposite effects on foam cell formation and protein markers expression.

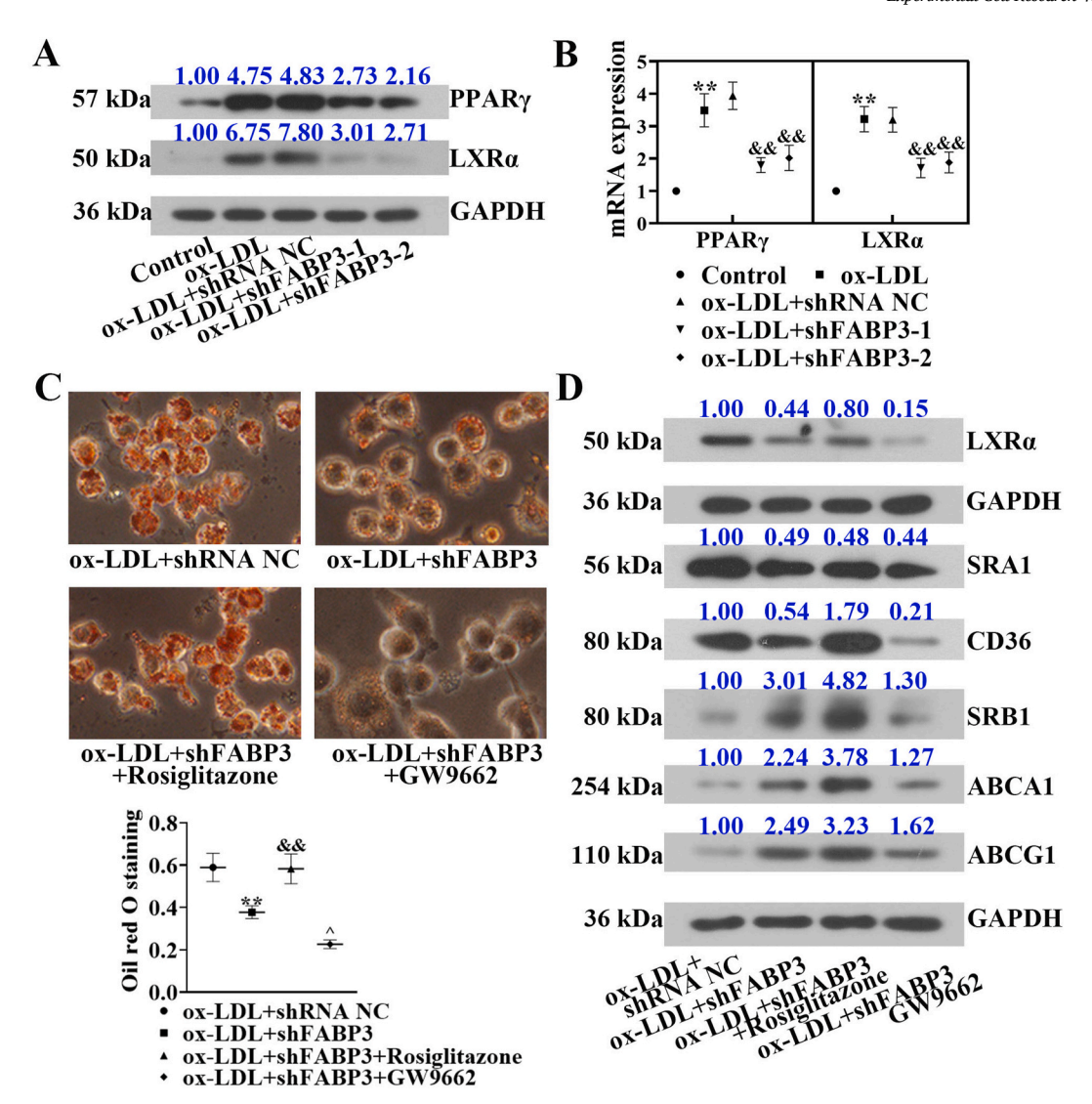


Fig. 4. Inhibition of FABP3 decreased foamy macrophage formation was related to the PPAR $\gamma$  signal pathway. Murine peritoneal macrophages were cultured in the special culture medium in a 5 % CO<sub>2</sub> atmosphere at 37 °C. Lentivirus carrying shFABP3 or shRNA NC were performed to infect the cells for 24 h and subsequently exposed with ox-LDL (50 μg/ml) and co-incubated with Rosiglitazone (1 μmol/L) or GW9662 (10 μmol/L) for 24 h. (A) Western blot and (B) qPCR were used to detect the expression of PPAR $\gamma$  and LXR $\alpha$  in macrophages. (C) Representative Oil Red O-stained images of macrophages and quantification of the staining. (D) Immunoblots of LXR $\alpha$ , SRA1, CD36, SRB1, ABCA1, and ABCG1 in macrophages. In Fig. 4B, \*\*p < 0.01 denote significant differences between the Control and the ox-LDL groups,  $^{\&\&}p$  < 0.01 denote significant differences between the ox-LDL + shRNA NC and ox-LDL + shFABP3 groups. In Fig. 4C, \*\*p < 0.01 denote significant differences between the ox-LDL + shFABP3 and ox-LDL an

# 4. Discussion

We here investigated the effects of FABP3 on atherosclerosis progression by using FABP3 shRNA lentivirus infection both in ApoE $^{-/-}$  mice in response to HFD and in murine peritoneal macrophages in response to ox-LDL. The expression of FABP3 was increased in HFD-fed ApoE $^{-/-}$  mice. Downregulation of FABP3 diminished atherosclerotic lesions and inhibited the accumulation of foamy macrophages, which was further related to PPAR $\gamma$ . Our results indicated the therapeutic promise of FABP3 inhibition to prevent atherogenesis.

Atherosclerosis is a complex pathological process that involves inflammatory response, endothelial dysfunction, and lipids accumulation in arteria [18]. Macrophage is one of the main cell types involved in atherosclerosis progression. In the course of atherosclerosis occurrence, high levels of cholesterol and saturated fatty acid result in the accumulation of lipid droplets in the subendothelium. Meanwhile, during inflammation or external stimulation, a growing number of macrophages migrate into the endothelial tissue and fill with lipid droplets form fatty streak, the earliest atherosclerotic lesion [19]. Subsequently, atherosclerotic plaques arise and are considered the occurrence of atherosclerosis [20]. HFD including cholesterol and pork fat that are rich in saturated fatty acid. Both cholesterol and saturated fatty acid lead to lipid droplets and macrophage foam cells, thus result in atherosclerosis [21]. In line with these features, atherosclerotic lesion formation and lipid deposition in atherosclerotic plaques were observed in the aorta of  ${\rm ApoE}^{-/\cdot}$  mice feeding with HFD over 12 weeks, which indicated an atherosclerosis mouse model was established successfully.

We next examined the expression of FABP3 in the aorta of ApoE $^{-/\cdot}$ mice. FABP3 is one of the lipid chaperones, which play a key role in lipid metabolic regulation and inflammatory responses. A report had indicated that the levels of FABP3 in serum were increased in nonalcoholic fatty liver disease patients [8]. Otherwise, the expression of FABP3 was elevated in LDL-treated mouse bone marrow-derived macrophages during foam cell formation [10]. In the present study, the FABP3 level was increased in the aorta of ApoE $^{-/\cdot}$ mice with HFD feeding, which was consistent with the previous research [8,10]. Moreover, FABPs were

related to cardiovascular risk and acted as adipokines in mediating adipocyte and macrophage interactions during inflammation [22]. The results of immunofluorescence in the present study showed that FABP3 was partly co-expressed with Mac-3, a biomarker of macrophages. These findings implied that FABP3 might act on macrophages and regulate atherosclerosis development.

Foam cell formation is strongly linked with the multiple factors in charge of cholesterol uptake and efflux. For instance, SRA1, CD36, SRB1, ABCA1, and ABCG1. SRA1 is a crucial molecule involved in cholesterol uptake by macrophages ingesting ox-LDL [23]. CD36 is a novel receptor that is abundantly present in lipid-loaded macrophages in the aorta of atherosclerotic patients [24]. In the process of cholesterol efflux, SRB1, ABCA1, and ABCG1 are transporters of HDL to acquire additional cholesterol from macrophages [25]. Li and co-authors demonstrated that overexpression of FABP3 elevated lipid deposition in the renal tubules of Bama minipigs fed with a high-fat/high-sucrose diet [26]. Downregulation of FABP3 notably decreased lipid droplet formation under hypoxia in glioblastoma cells and breast cancer cells [27]. Our results showed that knockdown of FABP3 significantly regulated the expression of lipid metabolism markers and eliminated the lipid deposition induced by ox-LDL in macrophages and ensuing inhibited foam cell formation. Furthermore, the atherosclerotic lesion and lipid deposition in plaques were less in FABP3 shRNA lentivirus infected HFD-fed ApoE<sup>-/-</sup> mice. The above results indicated that FABP3 silencing was endowed with quite evident anti-atherosclerotic effects.

Increasing studies reported that PPARy was connected with multiple diseases, such as inflammation, cardiovascular disease, and so on. Ajay had indicated that activation of PPARy promoted inflammation and aggravated atherosclerosis [28]. Sara and co-authors demonstrated that PPARy exerted a pro-atherogenic function, while macrophage nuclear receptor corepressors (NCOR) inhibited atherosclerosis by suppressing the PPARy signature [29]. Although several studies reported the pro-inflammatory actions and enhanced binding with ox-LDL of macrophage in PPARy, others suggested that PPARy had protective functions in atherogenesis [13]. Gwon et al. had shown that phenethyl isothiocyanate prominently promoted cholesterol transport reversing and inhibited the inflammation and lipid accumulation by acting PPARy [30]. In our study, PPARy agonist rosiglitazone removed the reduction of lipid deposition in macrophages induced by FABP3 silencing, whereas PPARy antagonist GW9662 had the opposite effect. Noteworthy, activation of PPARy not only upregulated the expression of CD36 but also elevated the levels of SRB1, ABCA1, and ABCG1, which indicated that PPARy had facilitation to both the uptake as well as the efflux of cholesterol in macrophages. Moreover, PPARy was reported to enhance the expression of FABP3 in skeletal muscle tissue under treatment of short-term starvation [31]. On the other hand, FABP3 increased the expression of PPARy to enhance lipid accumulation in dairy cow mammary epithelial cells [32]. These studies revealed an intricate interaction and cross-talk between FABP3 and PPARy. It appeared that FABP3 deficiency relieved atherosclerosis injury by inhibiting macrophage foam cell formation partly in the action of the PPARy signaling pathway. This raised an interesting possibility that some factors, involved in lipid metabolism, might exert functions between FABP3 and PPARy in atherosclerosis, which needed future studies. Moreover, polyunsaturated fatty acids (PUFA) were related to multiple diseases by regulating macrophage functions [33]. Unbalance of n-6 and n-3 PUFAs gave rise to cancer, autoimmune disorder, and cardiovascular disorders [34]. Reducing the n-6/n-3 PUFAs ratio decreased the expression of CD36 via the PPARy pathway thus suppressed the formation of macrophage foam cells [35]. One another challenge will be to investigate the connection between FABP3 and PUFAs.

#### 5. Conclusions

In summary, our data indicated that FABP3 was highly expressed in the aorta of HFD-fed  $ApoE^{-/-}$  mice. Silencing FABP3 attenuated

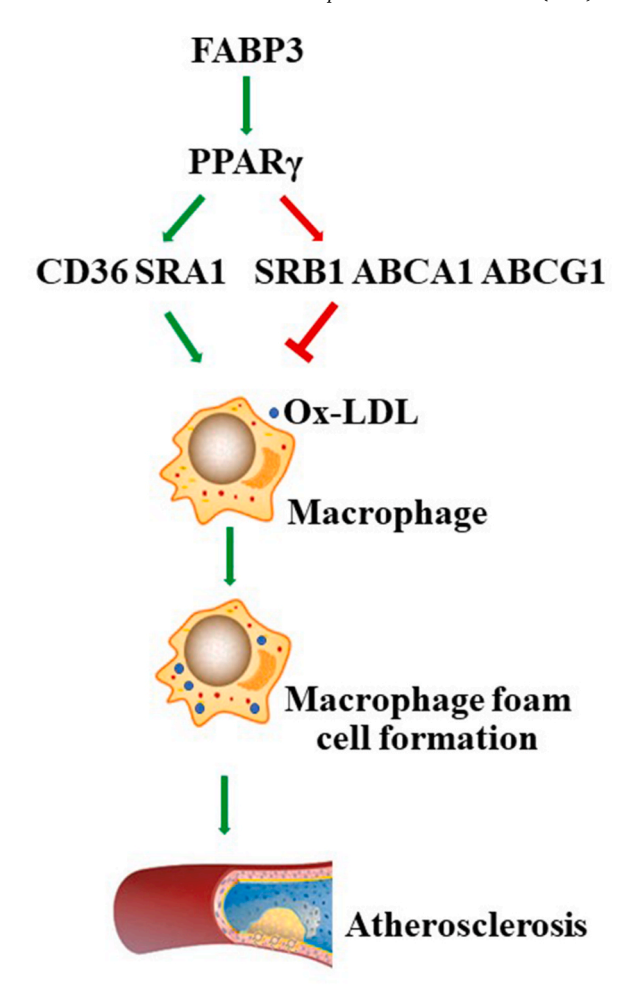


Fig. 5. Schematic diagram of the role of FABP3 on macrophage foam cell formation in atherosclerosis. FABP3 enhanced atherosclerosis on account of promoted macrophage foam cell formation partly via the PPARy signal pathway.

atherosclerosis due to decreased macrophage foam cell formation partly through inhibiting the PPAR $\gamma$  signal pathway. The functional cascade was displayed in Fig. 5. FABP3 inhibition might act a protective role in atherosclerosis which enlarged the window used for atherosclerosis therapy.

# Credit author statement

Lili Tan and Jie Lu: Conceptualization, Methodology, Data curation, Writing – original draft preparation; Lili Tan: Writing-Reviewing and Editing; Limin Liu: Methodology, Data curation; Lu Li: Validation, Supervision.

# **Declarations of competing interest**

The authors declare that they have no competing interests.

# Acknowledgements

This research was supported by grants from the National Natural Science Foundation of China (No. 82001492), the Guide Project for Key Research and Development Foundation of Liaoning Province (No. 2019010173-JH8/103), the Shenyang Science and Technology Project (No. 19-110-4-28) and the Guide Project for Key Research and Development Plan of Liaoning Province (2018) (No. 2018225015).

#### Appendix A. Supplementary data

Supplementary data to this article can be found online at https://doi.org/10.1016/j.yexcr.2021.112768.

#### References

- [1] N.D. LeBlond, J.R.C. Nunes, T.K.T. Smith, C. O'Dwyer, S. Robichaud, S. Gadde, M. Cote, B.E. Kemp, M. Ouimet, M.D. Fullerton, Foam cell induction activates AMPK but uncouples its regulation of autophagy and lysosomal homeostasis, Int. J. Mol. Sci. 21 (2020).
- [2] W.G. Robichaux 3rd, F.C. Mei, W. Yang, H. Wang, H. Sun, Z. Zhou, D.M. Milewicz, B.B. Teng, X. Cheng, Epac1 (exchange protein directly activated by cAMP 1) upregulates LOX-1 (oxidized low-density lipoprotein receptor 1) to promote foam cell formation and atherosclerosis development, Arterioscler. Thromb. Vasc. Biol. 40 (2020) e322–e335.
- [3] P. Shashkin, B. Dragulev, K. Ley, Macrophage differentiation to foam cells, Curr. Pharm. Des. 11 (2005) 3061–3072.
- [4] M.A.C. Depuydt, K.H.M. Prange, L. Slenders, T. Ord, D. Elbersen, A. Boltjes, S.C. A. de Jager, F.W. Asselbergs, G.J. de Borst, E. Aavik, T. Lonnberg, E. Lutgens, C. K. Glass, H.M. den Ruijter, M.U. Kaikkonen, I. Bot, B. Slutter, S.W. van der Laan, S. Yla-Herttuala, M. Mokry, J. Kuijer, M.P.J. de Winther, G. Pasterkamp, Microanatomy of the human atherosclerotic plaque by single-cell transcriptomics, Circ. Res. 127 (2020) 1437–1455.
- [5] R.K. Ockner, J.A. Manning, R.B. Poppenhausen, W.K. Ho, A binding protein for fatty acids in cytosol of intestinal mucosa, liver, myocardium, and other tissues, Science 177 (1972) 56–58.
- [6] M. Furuhashi, G.S. Hotamisligil, Fatty acid-binding proteins: role in metabolic diseases and potential as drug targets, Nat. Rev. Drug Discov. 7 (2008) 489–503.
- [7] K. Setsuta, Y. Seino, T. Ogawa, M. Arao, Y. Miyatake, T. Takano, Use of cytosolic and myofibril markers in the detection of ongoing myocardial damage in patients with chronic heart failure, Am. J. Med. 113 (2002) 717–722.
- [8] O. Basar, E. Akbal, S. Koklu, Y. Tuna, E. Kocak, N. Basar, D. Tok, H. Erbis, M. Senes, Increased H-FABP concentrations in nonalcoholic fatty liver disease. Possible marker for subclinical myocardial damage and subclinical atherosclerosis, Herz 38 (2013) 417–422.
- [9] A. Zamzam, M.H. Syed, J. Harlock, J. Eikelboom, K.K. Singh, R. Abdin, M. Qadura, Urinary fatty acid binding protein 3 (uFABP3) is a potential biomarker for peripheral arterial disease, Sci. Rep. 11 (2021) 11061.
- [10] Y.B. Shaik-Dasthagirisaheb, S. Mekasha, X. He, F.C. Gibson 3rd, R.R. Ingalls, Signaling events in pathogen-induced macrophage foam cell formation, Pathog. Dis. 74 (2016).
- [11] K. Chen, Q.J. Chen, L.J. Wang, Z.H. Liu, Q. Zhang, K. Yang, H.B. Wang, X.X. Yan, Z. B. Zhu, R. Du, R.Y. Zhang, W.F. Shen, L. Lu, Increment of HFABP level in coronary artery in-stent restenosis segments in diabetic and nondiabetic minipigs: HFABP overexpression promotes multiple pathway-related inflammation, growth and migration in human vascular smooth muscle cells, J. Vasc. Res. 53 (2016) 27–38.
- [12] M. Botta, M. Audano, A. Sahebkar, C.R. Sirtori, N. Mitro, M. Ruscica, PPAR agonists and metabolic syndrome: an established role? Int. J. Mol. Sci. 19 (2018).
- [13] P.D. Pelton, L. Zhou, K.T. Demarest, T.P. Burris, PPARgamma activation induces the expression of the adipocyte fatty acid binding protein gene in human monocytes, Biochem. Biophys. Res. Commun. 261 (1999) 456–458.
- [14] E. Wouters, E. Grajchen, W. Jorissen, T. Dierckx, S. Wetzels, M. Loix, M. P. Tulleners, B. Staels, P. Stinissen, M. Haidar, J.F.J. Bogie, J.J.A. Hendriks, Altered PPARgamma expression promotes myelin-induced foam cell formation in macrophages in multiple sclerosis, Int. J. Mol. Sci. 21 (2020).
- [15] M. Boss, M. Kemmerer, B. Brune, D. Namgaladze, FABP4 inhibition suppresses PPARgamma activity and VLDL-induced foam cell formation in IL-4-polarized human macrophages, Atherosclerosis 240 (2015) 424–430.
- [16] Q. Meng, M. Ma, W. Zhang, Y. Bi, P. Cheng, X. Yu, Y. Fu, Y. Chao, T. Ji, J. Li, Q. Chen, Q. Zhang, Y. Li, J. Shan, H. Bian, The gut microbiota during the progression of atherosclerosis in the perimenopausal period shows specific compositional changes and significant correlations with circulating lipid metabolites, Gut Microb. 13 (2021) 1–27.

- [17] Y. Luo, K. Tanigawa, A. Kawashima, Y. Ishido, N. Ishii, K. Suzuki, The function of peroxisome proliferator-activated receptors PPAR-gamma and PPAR-delta in Mycobacterium leprae-induced foam cell formation in host macrophages, PLoS Neglected Trop. Dis. 14 (2020), e0008850.
- [18] J.X. Sun, C. Zhang, Z.B. Cheng, M.Y. Tang, Y.Z. Liu, J.F. Jiang, X. Xiao, L. Huang, Chemerin in atherosclerosis, Clin. Chim. Acta 520 (2021 Sep) 8–15, https://doi. org/10.1016/j.cca.2021.05.015.
- [19] P. Lin, H.H. Ji, Y.J. Li, S.D. Guo, Macrophage plasticity and atherosclerosis therapy, Front. Mol. Biosci. 8 (2021) 679797.
- [20] J. Bonetti, A. Corti, L. Lerouge, A. Pompella, C. Gaucher, Phenotypic modulation of macrophages and vascular smooth muscle cells in atherosclerosis-nitro-redox interconnections, Antioxidants 10 (2021).
- [21] D.A. Chistiakov, Y.V. Bobryshev, A.N. Orekhov, Macrophage-mediated cholesterol handling in atherosclerosis, J. Cell Mol. Med. 20 (2016) 17–28.
- [22] A.E. Thumser, J.B. Moore, N.J. Plant, Fatty acid binding proteins: tissue-specific functions in health and disease, Curr. Opin. Clin. Nutr. Metab. Care 17 (2014) 124–129.
- [23] B.K. Ooi, B.H. Goh, W.H. Yap, Oxidative stress in cardiovascular diseases: involvement of Nrf2 antioxidant redox signaling in macrophage foam cells formation, Int. J. Mol. Sci. 18 (2017).
- [24] A. Nakata, Y. Nakagawa, M. Nishida, S. Nozaki, J. Miyagawa, T. Nakagawa, R. Tamura, K. Matsumoto, K. Kameda-Takemura, S. Yamashita, Y. Matsuzawa, CD36, a novel receptor for oxidized low-density lipoproteins, is highly expressed on lipid-laden macrophages in human atherosclerotic aorta, Arterioscler. Thromb. Vasc. Biol. 19 (1999) 1333–1339.
- [25] K.R. Feingold, Introduction to lipids and lipoproteins, in: K.R. Feingold, B. Anawalt, A. Boyce, G. Chrousos, W.W. de Herder, K. Dhatariya, K. Dungan, A. Grossman, J.M. Hershman, J. Hofland, S. Kalra, G. Kaltsas, C. Koch, P. Kopp, M. Korbonits, C.S. Kovacs, W. Kuohung, B. Laferrere, E.A. McGee, R. McLachlan, J. E. Morley, M. New, J. Purnell, R. Sahay, F. Singer, C.A. Stratakis, D.L. Trence, D. P. Wilson (Eds.), Endotext, South Dartmouth (MA), 2000.
- [26] L. Li, Z. Zhao, J. Xia, L. Xin, Y. Chen, S. Yang, K. Li, A long-term high-fat/high-sucrose diet promotes kidney lipid deposition and causes apoptosis and glomerular hypertrophy in Bama minipigs, PloS One 10 (2015), e0142884.
- [27] K. Bensaad, E. Favaro, C.A. Lewis, B. Peck, S. Lord, J.M. Collins, K.E. Pinnick, S. Wigfield, F.M. Buffa, J.L. Li, Q. Zhang, M.J.O. Wakelam, F. Karpe, A. Schulze, A. L. Harris, Fatty acid uptake and lipid storage induced by HIF-1alpha contribute to cell growth and survival after hypoxia-reoxygenation, Cell Rep. 9 (2014) 349–365.
- [28] A. Chawla, Control of macrophage activation and function by PPARs, Circ. Res. 106 (2010) 1559–1569.
- [29] S. Oppi, S. Nusser-Stein, P. Blyszczuk, X. Wang, A. Jomard, V. Marzolla, K. Yang, S. Velagapudi, L.J. Ward, X.M. Yuan, M.A. Geiger, A.T. Guillaumon, A. Othman, T. Hornemann, Z. Rancic, D. Ryu, M.H. Oosterveer, E. Osto, T.F. Luscher, S. Stein, Macrophage NCOR1 protects from atherosclerosis by repressing a pro-atherogenic PPARgamma signature, Eur. Heart J. 41 (2020) 995–1005.
- [30] M.H. Gwon, Y.S. Im, A.R. Seo, K.Y. Kim, H.R. Moon, J.M. Yun, Phenethyl isothiocyanate protects against high fat/cholesterol diet-induced obesity and atherosclerosis in C57BL/6 mice, Nutrients 12 (2020).
- [31] D. Holst, S. Luquet, V. Nogueira, K. Kristiansen, X. Leverve, P.A. Grimaldi, Nutritional regulation and role of peroxisome proliferator-activated receptor delta in fatty acid catabolism in skeletal muscle, Biochim. Biophys. Acta 1633 (2003) 43–50.
- [32] M.Y. Liang, X.M. Hou, B. Qu, N. Zhang, N. Li, Y.J. Cui, Q.Z. Li, X.J. Gao, Functional analysis of FABP3 in the milk fat synthesis signaling pathway of dairy cow mammary epithelial cells, In Vitro Cell. Dev. Biol. Anim. 50 (2014) 865–873.
- [33] L. Menegaut, A. Jalil, C. Thomas, D. Masson, Macrophage fatty acid metabolism and atherosclerosis: the rise of PUFAs, Atherosclerosis 291 (2019) 52–61.
- [34] S. Marventano, P. Kolacz, S. Castellano, F. Galvano, S. Buscemi, A. Mistretta, G. Grosso, A review of recent evidence in human studies of n-3 and n-6 PUFA intake on cardiovascular disease, cancer, and depressive disorders: does the ratio really matter? Int. J. Food Sci. Nutr. 66 (2015) 611–622.
- [35] Z. Song, H. Xia, L. Yang, S. Wang, G. Sun, Lowering the n-6/n-3 PUFAs ratio inhibits the formation of THP-1 macrophage-derived foam cell, Lipids Health Dis. 17 (2018) 125.